Vortices and 2D Bosons: A Path-Integral Monte Carlo Study

Henrik Nordborg* and Gianni Blatter

Theoretische Physik, ETH-Hönggerberg, CH-8093 Zürich, Switzerland
(Received 2 December 1996)

The vortex system in a high-T_c superconductor has been studied numerically using the mapping to 2D bosons and the path-integral Monte Carlo method. We find a single first-order transition from an Abrikosov lattice to an entangled vortex liquid. The transition is characterized by an entropy jump $\Delta S \approx 0.4 k_B$ per vortex and layer (parameters for YBa$_2$Cu$_3$O$_7$) and a Lindemann number $c_L \approx 0.25$. The increase in density at melting is given by $\Delta \rho \approx 6.0 \times 10^{-4}/\lambda(T)^2$. The vortex liquid corresponds to a bosonic superfluid, with $\rho_s = \rho$ even in the limit $\lambda \to \infty$.   [S0031-9007(97)03960-4]

PACS numbers: 74.60.Ec, 05.30.Jp, 74.20.De

Our understanding of the phase diagram of type II superconductors has improved significantly since the mixed state was introduced by Abrikosov in 1957 [1]. The vortex state is of particular interest for the high-T_c superconductors, where strong thermal fluctuations lead to melting of the vortex lattice and the appearance of a vortex liquid phase. Experimental evidence for a first-order vortex lattice melting transition has been obtained from the observation of jumps in the resistivity and in the magnetization [2–4]. More recently, the latent heat of the transition has been measured directly in an untwinned YBa$_2$Cu$_3$O$_7$ (YBCO) single crystal [5]. Theoretically, vortex lattice melting has been studied using various approximate techniques, including the renormalization group, perturbative expansions, density functional theory, and the Lindemann criterion [6]. The absence of one simple and reliable theory has provoked large interest in numerical simulations. A number of models, such as the 3D frustrated XY model, the lattice London model, and the lowest Landau level approximation, have been used, with no consistent picture emerging, however [7]. A careful analysis of the 3D vortex system has been carried out by Šášik and Stroud [8], using the lowest Landau level approximation at constant *applied* field. They obtained a jump in the magnetization and could accurately trace the first-order melting transition in YBCO.

A very fruitful concept was introduced by Nelson [9], who showed that the classical statistical mechanics of the vortex system can be mapped onto the quantum statistical mechanics of a 2D system of Yukawa bosons, i.e., bosons interacting with the potential $V(R) = g^2 K_0(R/\lambda)$, where K_0 is a modified Bessel function, λ is the London penetration depth, and g^2 is a coupling constant to be defined below. We will refer to this system as the Bose model of the vortex system. A consequence of this mapping is the prediction of a melting transition into an *entangled* vortex liquid, corresponding to a lattice to superfluid transition in the Bose system. Unfortunately, perturbation theory does not work for strongly interacting 2D bosons, and the only quantitative results are from ground-state Monte Carlo simulations [10], which have not studied the superfluid

density or the excitation spectrum. In this Letter, we present the first path-integral Monte Carlo results for 2D Yukawa bosons. Both the cases λ finite and $\lambda = \infty$ (2D Bose Coulomb liquid) are considered. The results are interpreted for the solid-liquid transition in the vortex system.

In the Feynman path-integral formulation, a d-dimensional system of massive quantum particles is equivalent to a classical $(d + 1)$-dimensional system of interacting elastic strings. The dimensionless imaginary-time action for N Yukawa bosons is given by

$$S/\hbar = \int_0^\beta d\tau \left\{ \sum_i \frac{1}{2\Lambda^2} \left(\frac{d\mathbf{R}_i}{d\tau} \right)^2 + \sum_{i<j} K_0 \left(\frac{R_{ij}}{\lambda} \right) \right\},$$
(1)

where all energies are measured in units of g^2 and all lengths in units of the particle distance a_0 in the crystal, $a_0^2 = 2/\rho\sqrt{3}$, with ρ being the density. The de Boer parameter Λ, $\Lambda^2 = \hbar^2/m a_0^2 g^2$, measures the size of quantum fluctuations, $\beta = g^2/T^B$ is the inverse temperature, and the $\mathbf{R}_i$ denote the particle positions. The partition function is the sum over all world lines weighted by this action and subject to the boundary conditions $\mathbf{R}_i(\beta) = \mathbf{R}_j(0)$; i.e., every line ends on itself or on some other line. This action is also valid in the limit $\lambda \to \infty$ if a uniform background charge is subtracted. In this case, the Bessel function reduces to a logarithm.

Redefining parameters, Eq. (1) can be interpreted as the free energy for the vortex system in a type II superconductor, $S/\hbar = \mathcal{F}/T$ [9], with

$$\Lambda = \frac{T}{a_0 \sqrt{2\varepsilon_l \varepsilon_0}}, \qquad \beta = \frac{2\varepsilon_0 L_z}{T},$$
(2)

where T is the temperature of the vortex system and L_z is the thickness of the sample. For an anisotropic superconductor, the elasticity is $\varepsilon_l \approx \varepsilon^2 \varepsilon_0$, where $\varepsilon^2 = m/M < 1$ is the anisotropy parameter. Two approximations are required for this mapping from bosons to vortices. First, the original London functional for the free energy contains retarded and advanced interactions between the vortex lines, which are mediated by gauge fields in the Bose

picture [11]. Here, retardation is neglected, equivalent to keeping only the first term in an expansion around straight lines. Second, it has been argued that vortex loops in the *ab* planes are important for vortex lattice melting [12]. A simple estimate for the free energy of a loop of length L, $\mathcal{F} \approx (L/\xi)(\varepsilon\varepsilon_0\xi - T \ln 3)$, shows that loops proliferate in the critical regime close to H_{c2}. We do not consider the critical regime in this work.

The phase diagram for the Bose model, shown schematically in Fig. 1, contains three phases: a classical high temperature normal liquid phase, a crystal for low temperatures and small quantum effects, and a superfluid as quantum effects start to dominate at low temperatures. This can be understood by considering the three energy scales involved. The transition from a normal liquid to a lattice is determined by the competition between the *thermal* energy $T^B = g^2/\beta$ and the *potential* energy g^2. In the limit $\lambda \to \infty$ and $\Lambda = 0$, the transition takes place at $\beta_m \approx 140$ [13]. With increasing quantum effects, we find a transition from a normal liquid to a superfluid when the thermal energy matches the *kinetic* energy, $\Lambda^2\beta \approx 1$. At low temperatures, the competition between potential and kinetic energies determines whether the system is a crystal or a superfluid. For $\beta, \lambda = \infty$, it is known that $\Lambda_m \approx 0.062$ [10].

The boson phase diagram can be reinterpreted in terms of the vortex system, where β is proportional to the sample thickness and Λ measures the strength of *thermal* fluctuations. For thin samples, $\beta < \beta_m, 1/\Lambda^2$, we find a *disentangled* vortex liquid. In thicker samples, the system is either a lattice or an *entangled* vortex liquid, depending on temperature and magnetic field. Note the nontrivial mapping between the *H*-*T* and Λ-β phase diagrams. In a thin sample, the constant field line (dash-dotted in Fig. 1) passes through the crystalline phase (low T), the disentangled liquid phase (intermediate T), and the entangled liquid phase (high T). With increasing L_z, this line moves to higher values of β, and the vortex lattice melting line is determined solely by the value of Λ_m.

The simulations are carried out using the path integral Monte Carlo technique, which is exact for bosons [14]. Typical runs involve $N = 64$ world lines, though systems as large as $N = 100$ have been used for analyzing finite-size effects. With $\beta = 300$ we accurately capture the ground-state behavior; e.g., we reproduce the $T^B = 0$ result of Ref. [10] to within less than 1%. We find that $M = 100$ Trotter slices are sufficient to eliminate systematic errors in the bosonic quantum phase transition; see Ref. [19] for details. For the largest systems we used roughly 30 000 sweeps to equilibrate and 80 000 sweeps to measure.

The lattice to liquid transition is identified through the vanishing of the first Bragg peak ($\mathbf{Q} = \mathbf{Q}_1, \tau = 0$) in the structure factor

$$S(\mathbf{Q}, \tau) = \frac{1}{N} \langle \rho_\mathbf{Q}(\tau)\rho_{-\mathbf{Q}}(0) \rangle, \qquad (3)$$

where $\rho_\mathbf{Q}(\tau)$ is the partial Fourier transform of the density operator, $\rho(\mathbf{R}, \tau) = \sum_i \delta[\mathbf{R} - \mathbf{R}_i(\tau)]$. The superfluid density of the Bose system is measured using the winding number [14],

$$\frac{\rho_s}{\rho} = \frac{\langle \mathbf{W}^2 \rangle}{2\Lambda^2\beta N}, \qquad (4)$$

with the winding vector $\mathbf{W} = \sum_i \int_0^\beta d\tau\, \partial_\tau \mathbf{R}_i$ measuring the diffusion of the center-of-mass of the system in imaginary time. As the equilibration of the winding number is very slow for large systems, we use systems with $N = 36$ to compute the superfluid density. For larger systems, we define the parameter ρ_e according to

$$\frac{\rho_e}{\rho} = \frac{\text{entangled lines}}{\text{total number of lines}}, \qquad (5)$$

where a line is *entangled* if it does not end on itself, $\mathbf{R}_i(\beta) \neq \mathbf{R}_i(0)$. The parameter ρ_e measures the importance of quantum effects in the system, and is therefore *related* to superfluidity. We emphasize, however, that ρ_e is *not* the superfluid density.

We begin by considering the incompressible case with $\lambda = \infty$. In Fig. 2 we show the results for the first Bragg peak and the parameter ρ_e. The lattice disappears in a sharp transition at $\Lambda_m \approx 0.062$, in perfect agreement with ground-state simulations of the same model [10]. The height of the Bragg peak is related to the Lindemann number according to $S(Q_1) = N \exp(-8\pi^2 c_L^2/3)$, and we find $c_L \approx 0.25$. Using Eq. (2), we obtain the melting line

$$B_m(T) = \frac{4\Lambda_m^2\Phi_0}{\sqrt{3}} \frac{\varepsilon_l\varepsilon_0}{T^2}, \qquad (6)$$
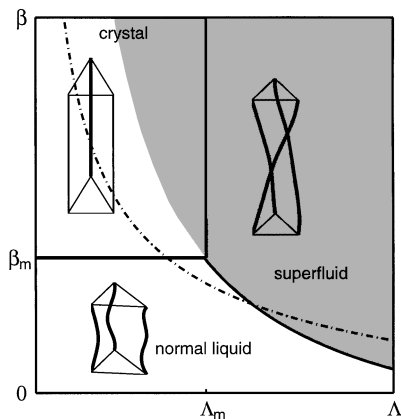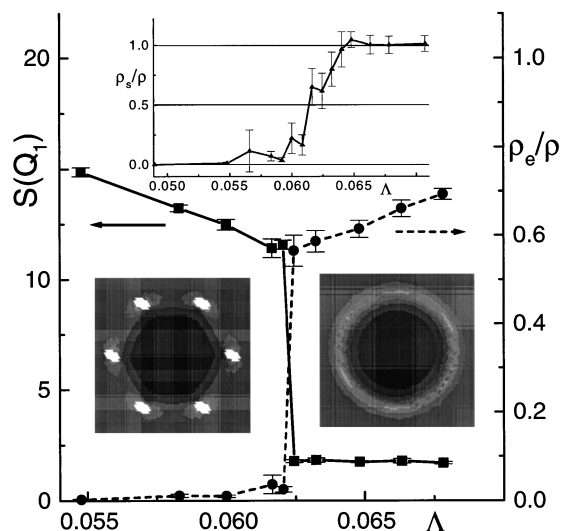

FIG. 1. Schematic phase diagram for a system of 2D charged bosons in terms of Λ and β. The solid lines represent phase transitions, and quantum effects are relevant in the shaded region. In the vortex system, the parameters map to $\Lambda^2 = T^2/2\varepsilon_l\varepsilon_0 a_0^2$ and $\beta = 2\varepsilon_0 L_z/T$. The constant field line for a thin sample ($L_z < 70T/\varepsilon_0$) is shown (dash-dotted) as it runs through all three phases. For thicker samples, this line is pushed upward.

FIG. 2.   The first Bragg peak and the entanglement parameter ρ_e for a system with 64 lines and $\beta = 300$. A sharp transition from a crystal to an entangled liquid is found at $\Lambda_m = 0.062$. The structure factors just before and after the melting transition are displayed. The inset shows the superfluid density for a system with 36 lines.

as expected from a Lindemann criterion with $\Lambda_m \propto c_L^2$ [11], giving good agreement with experimental results on YBCO. Its universal character applies only to large magnetic fields; the finiteness of λ leads to a reentrant melting line at low fields [15].

If the vortex lattice melts in a single transition, symmetry requires it to be first order [16]. In Fig. 3, we plot the energy per line and unit length $e \equiv \langle \mathcal{F} \rangle / NL_z$. The corresponding energy of the vortex system is defined as $e_\phi \equiv T^2 \partial_T \ln \mathcal{Z} / NL_z$, with $\mathcal{Z}$ the partition function [17]. Using the scaling form $\mathcal{F} = \varepsilon_0 a_0 f[\{R_{ij}/a_0\}]$, valid for large λ, we obtain $e_\phi = e(1 + t^2)/(1 - t^2)$, where $t = T/T_c$. The jump in entropy at the transition is given by
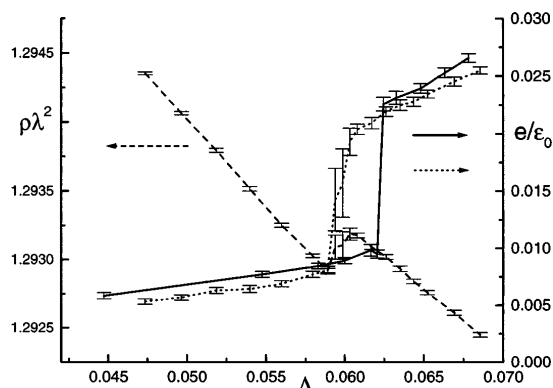

FIG. 3.   The energy e per line of the vortex system (right axis) for $\lambda = \infty$ (solid line) and $\lambda \approx 1.06a_0$ (dotted line). The energy of a perfect lattice with the same density has been subtracted in both cases. In the compressible system the transition shows a jump in the density (left axis, dashed line). Note the (small) shift in Λ_m as the interaction range is reduced.

$T_m \Delta s_\phi = \Delta e_\phi$. From Fig. 3 we obtain $\Delta e \approx 0.015\varepsilon_0$ and therefore

$$\Delta s[k_B/\text{length}] \approx 0.03\varepsilon_0(0)/T_m . \tag{7}$$

Using parameters for YBCO (layer separation $d = 12$ Å, $\lambda_{ab} \approx 1400$ Å, and $T_m \approx T_c$), we obtain $\Delta s_\phi \approx 0.4k_B$ per vortex and layer, which compares favorably with the experimental result of $\Delta s_\phi \approx 0.45k_B$ [5].

For the compressible case with λ finite, the statistical attraction between the bosons produces an increase of the density upon melting. This maps to a densified vortex liquid due to the entanglement of the flux lines [18]. In order to study this effect, we have developed an isobaric Monte Carlo algorithm which allows us to fix the external pressure and let the volume adjust [19]. The results are shown in Fig. 3 for a system with $\lambda \approx 1.06a_0$. The transition is shifted to a slightly smaller value of Λ_m due to the weaker interaction between the lines. The small shift, less than 4%, shows that Eq. (6) gives a good description of the melting for a large range of fields. The change in density depends on the value of λ/a_0; in the present case $\Delta\rho/\rho \approx 0.0003$, which is consistent with the result (7) via the Clausius-Clapeyron relation, $\Delta e/\varepsilon_0 = 8\pi\Delta\rho\lambda^2(T)^2$.

We turn to the discussion of the liquid phase. In Fig. 2 we show the entanglement parameter ρ_e which rises sharply at the transition, indicating that the vortex liquid entangles *immediately* upon melting. This result is in agreement with recent flux transformer experiments, showing that the vortex correlation along the magnetic field disappears at the melting transition [20]. The possibility of a *disentangled* vortex liquid has attracted much interest in recent years [21]. Two theoretical arguments have been put forward in favor of the existence of this phase. To begin with, the melting of the vortex lattice into an entangled vortex liquid involves the change of two symmetries: The transverse translational symmetry of the lattice and the longitudinal gauge symmetry. If these two symmetries do not change simultaneously, an intermediate phase will appear. A second argument stems from the analysis of the 2D Bose Coulomb liquid. It can be shown that the suppression of long wavelength density fluctuations in this system leads to enhanced phase fluctuations and an algebraic decay of the off-diagonal long-range order (ODLRO) even in the ground state ($T^B = 0$) [10]. However, the absence of a $T^B = 0$ Bose condensate has no straightforward implication for the superfluid density, which is related to the excitation spectrum rather than to the ground-state properties. In the inset of Fig. 2 we show the superfluid density measured by the winding number. Apart from a slight broadening of the transition due to the smaller system size, the result shows that $\rho_s = \rho$ as soon as the translational symmetry is restored in the liquid. Retardation may modify this result in the following ways: (i) The decrease in the effective mass of the bosons (elastic tension of the vortices) favors the entangled state. (ii) The retardation may render the entanglement unstable, thereby favoring a
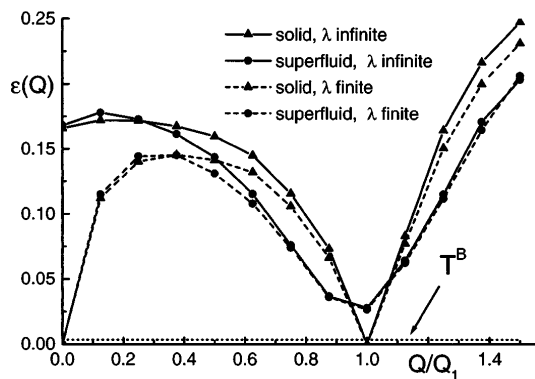
FIG. 4.   The excitation spectra $\varepsilon(Q)$ in units of g^2 for a system of 64 lines. Increasing the range λ of the interaction shifts the sound mode to the plasma frequency, but leaves the roton minimum unchanged. The latter collapses upon crystallization.

disentangled liquid. Thus, the question regarding the possibility of a disentangled liquid phase in the retarded model has not been completely settled.

Additional information on the properties of the Bose superfluid/vortex liquid is provided through the analysis of the dynamic structure factor. Following Nelson [9], the partial Fourier transform $S(Q, \tau)$ takes the form $S(Q, \tau) \approx S(Q, 0) \exp\{-\varepsilon(Q)|\tau|\}$, where $\varepsilon(Q)$ is the excitation spectrum of the Bose system. Thus, the bosonic excitation spectrum defines a longitudinal correlation length $l_r = T/2\Delta_r \varepsilon_0$ in the vortex fluid, where Δ_r denotes the roton minimum. We compute the excitation spectrum from our simulations by fitting the measured $S(Q, \tau)$ to the single mode approximation,

$$S(Q, i\omega_n) = \frac{C(Q)}{[\omega_n + \Gamma(Q)]^2 + \varepsilon(Q)^2}, \qquad (8)$$

where $\varepsilon(Q)$ and $\Gamma(Q)$ are the energy and inverse lifetime of the excitations. In Fig. 4 we show the resulting spectra both for the incompressible ($\lambda = \infty$) and the compressible ($\lambda < \infty$) fluids. Most interestingly, the phonon branch at small Q turns into a plasmon branch as $\lambda \to \infty$, while the roton minimum undergoes no visible change. From the roton minimum $\Delta_r \approx 0.027$, we determine the correlation or entanglement length at the melting transition, $l_r \approx 1.6 a_0 \sqrt{\varepsilon_l/\varepsilon_0}$, *independent* of the interaction range λ. Note that in our simulations the roton gap is much larger than the temperature and we expect to probe the ground state behavior of the system.

In conclusion, our simulation of the 2D Coulomb Bose model reveals a single $T^B \approx 0$ quantum phase transition from a crystal to a superfluid phase at $\Lambda_m \approx 0.062$. This translates to a first-order melting transition of the Abrikosov vortex lattice into an entangled vortex liquid phase. The long-range interaction changes the bosonic excitation spectrum from phonons to plasmons for small Q, but does not modify the roton minimum. We find that superfluidity is stable against static long-range interactions.

*Present address: Material Science Division, Argonne National Laboratory, Argonne, IL 60439.
[1]   A. Abrikosov, Sov. Phys. JETP **5**, 1174 (1957).
[2]   H. Pastoriza *et al.,* Phys. Rev. Lett. **72**, 2951 (1994).
[3]   E. Zeldov *et al.,* Nature (London) **375**, 373 (1995).
[4]   U. Welp *et al.,* Phys. Rev. Lett. **76**, 4809 (1996).
[5]   A. Schilling *et al.,* Nature (London) **382**, 791 (1996).
[6]   E. Brezin *et al.,* Phys. Rev. B **31**, 7124 (1985); D. R. Nelson and H. S. Seung, Phys. Rev. B **39**, 9153 (1989); A. Houghton *et al.,* Phys. Rev. B **40**, 6763 (1989); S. Hikami *et al.,* Phys. Rev. B **44**, 10400 (1991); S. Sengupta *et al.,* Phys. Rev. Lett. **67**, 3444 (1991).
[7]   R. E. Hetzel *et al.,* Phys. Rev. Lett. **69**, 518 (1992); Y.-H. Li and S. Teitel, Phys. Rev. B **47**, 359 (1993); T. Chen and S. Teitel, Phys. Rev. Lett. **74**, 2792 (1995); G. Carneiro, Phys. Rev. Lett. **75**, 521 (1995); A. K. Nguyen *et al.,* Phys. Rev. Lett. **77**, 1592 (1996).
[8]   R. Šášik and D. Stroud, Phys. Rev. Lett. **75**, 2582 (1995).
[9]   D. R. Nelson, Phys. Rev. Lett. **60**, 1973 (1988); D. R. Nelson and H. S. Seung, Phys. Rev. B **39**, 9153 (1989).
[10] W. R. Magro and D. M. Ceperley, Phys. Rev. Lett. **73**, 826 (1994).
[11] G. Blatter *et al.,* Rev. Mod. Phys. **66**, 1125 (1994).
[12] A. K. Nguyen *et al.,* Phys. Rev. Lett. **77**, 1592 (1996).
[13] J. M. Caillol *et al.,* J. Stat. Phys. **28**, 325 (1982).
[14] D. M. Ceperley, Rev. Mod. Phys. **67**, 279 (1995).
[15] G. Blatter *et al.,* Phys. Rev. B **54**, 72 (1996).
[16] L. D. Landau, Phys. Z. Sowiet **11**, 26 (1937); S. Alexander and J. McTague, Phys. Rev. Lett. **41**, 702 (1978).
[17] The relevance of the temperature dependence of the Ginzburg-Landau parameters was pointed out by J. Hu and A. MacDonald, Phys. Rev. B **56**, 2788 (1997).
[18] D. R. Nelson, Nature (London) **375**, 356 (1995).
[19] H. Nordborg and G. Blatter (to be published).
[20] D. López *et al.,* Phys. Rev. Lett. **76**, 4034 (1996).
[21] M. V. Feigel'man *et al.,* Phys. Rev. B **48**, 16641 (1993); T. Chen and S. Teitel, Phys. Rev. Lett. **76**, 714 (1996).